

# Non-Stationary Covariance Functions for Spatial Data on Linear Networks

Alfredo Alegría

*Department of Statistics, Pontificia Universidad Católica de Chile, Avenida Vicuña Mackenna 4860, Macul, 7820436, Santiago, Chile*

---

## Abstract

We introduce a novel class of non-stationary covariance functions for random fields on linear networks that allows both the variance and the correlation range of the random field to vary spatially. The proposed covariance functions are useful to model random fields with a spatial dependence that is locally isotropic with respect to the resistance metric, a distance that reflects the topology of the network. We assess the statistical and computational performance of a weighted local likelihood estimator for the proposed models using synthetic data generated on the street network of the University of Chicago neighborhood.

*Keywords:* Generalized Stieltjes functions, Laplacian matrix, Log Gaussian Cox process, Positive definite functions, Gaussian random field, Resistance metric, Weighted local likelihood

---

## 1. Introduction

Data indexed by locations on a network arise naturally in a variety of applications, including processes on road, river, and electrical networks. Recent developments in the theory and methods of spatial statistics on linear networks can be found in Ver Hoef and Peterson (2010), Baddeley et al. (2017), Anderes et al. (2020), Cronie et al. (2020), Moradi and Mateu (2020), Baddeley et al. (2021), Porcu et al. (2023), Bolin et al. (2024), Møller and Rasmussen (2024), Moradi and Sharifi (2024), González-Pérez et al. (2025) and Alegría et al. (2026).

Specifically, a linear network  $\mathcal{L}$  is the union  $\mathcal{L} = \bigcup_{i=1}^m \ell_i$  of closed line segments  $\ell_1, \dots, \ell_m$  in  $\mathbb{R}^2$ , with  $m < \infty$ . Each segment has positive finite length and intersects other segments only at endpoints. Throughout, the network is assumed to be path-connected.

A second-order Gaussian random field (GRF)  $\{X(s) : s \in \mathcal{L}\}$  is completely characterized by its mean function, which we assume to be zero for simplicity, and by its covariance function  $K(s, t) = \text{cov}[X(s), X(t)]$ ,  $s, t \in \mathcal{L}$ . The construction of valid and versatile covariance functions is challenging because of the requirement that the covariance matrix of  $(X(s_1), \dots, X(s_N))^\top$ , given by

$$\boldsymbol{\Sigma} = [K(s_i, s_j)]_{i,j=1}^N,$$

---

*Email address:* `alfredo.alegría@uc.cl` (Alfredo Alegría)

should be positive semidefinite, for all  $N \in \mathbb{N}$  and for all collection of sites  $s_1, \dots, s_N \in \mathcal{L}$ . In other words,  $K$  must be a positive semidefinite function. The spectral theory of random fields on Euclidean spaces is useful to check for positive definiteness of a candidate function (see, e.g., [Yaglom, 1987](#)). In the network setting, however, analogous characterizations are unavailable.

It is commonly assumed that the covariance function is isotropic, meaning that there exists a function  $C : [0, \infty) \rightarrow \mathbb{R}$  such that

$$K(s, t) = C(d(s, t)), \quad s, t \in \mathcal{L},$$

with  $d(\cdot, \cdot)$  standing for a distance metric on  $\mathcal{L}$ . In practice, treating network coordinates as ordinary Euclidean coordinates can distort the proximity between locations and produce unrealistic results. To address this, [Anderes et al. \(2020\)](#) established positive definiteness for certain classes of isotropic covariance functions under the resistance metric (an extension of the resistance metric from electrical network theory) and showed that, under the geodesic (shortest-path) metric, these classes are valid only under restrictive assumptions on the network structure. Both the resistance and geodesic metrics, unlike the Euclidean metric, take the network topology into account.

Although isotropy is a convenient assumption, it can be overly restrictive. In geostatistical applications, there is increasing demand for more flexible models, particularly when analyzing data over large domains where the properties of the process may vary across space. See [Bolin et al. \(2025\)](#) for a recent development of non-stationary random fields on metric graphs formulated as solutions to stochastic partial differential equations, and an application to traffic speed data. In the context of log Gaussian Cox processes (LGCPs) ([Cox, 1955](#)), where the intensity of point occurrences is governed by a log Gaussian random field, isotropy of the underlying GRF prevents the number of points and the spatial extent of point clusters from varying across the domain. This limitation has been studied for point processes in Euclidean spaces by [Dvořák et al. \(2019\)](#). Similar issues arise on linear networks, as discussed by [Baddeley et al. \(2017\)](#), encouraging the development of more flexible models.

Motivated by this, we propose a general class of non-stationary covariance functions on linear networks, that is, covariance functions not solely determined by distance. The proposed covariance models allow both the variance and the correlation range of the random field to vary across the network, providing a network analogue of models previously proposed in Euclidean spaces ([Paciorek, 2003](#); [Paciorek and Schervish, 2006](#); [Anderes and Stein, 2011](#); [Kleiber and Nychka, 2012](#); [Mateu et al., 2013](#); [Liang and Marcotte, 2016](#)). Our framework produces covariance functions that are locally isotropic with respect to the resistance metric, ensuring interpretability and alignment with the topology of the network.

We exploit the connection between the proposed covariance functions and the class of generalized Stieltjes functions (see [Koumardos and Pedersen, 2019](#); [Menegatto, 2020](#) for a detailed treatment) to provide examples of non-stationary covariance functions in closed form.

To address statistical inference, we revisit the weighted local likelihood approach, originally introduced by [Anderes and Stein \(2011\)](#) for Euclidean spaces, and adapt it to the network setting. We then conduct a simulation study using synthetic data generated on the street network of the University of Chicago neighborhood, in which we estimate the local correlation range, examine the behavior of the method under different weighting schemes, and evaluate its computational performance.

The paper is organized as follows. Section 2 reviews the definition and properties of the resistance metric for linear networks. Section 3 presents the main theorem, examples, and illustrations. Section 4 describes the weighted local likelihood method and reports the results of the simulation study. Section 5 concludes the paper with a discussion and directions for future research.

## 2. Resistance metric

This section reviews the definition and properties of the resistance metric introduced in [Anderes et al. \(2020\)](#), as this metric is essential for building the non-stationary covariance functions proposed in this work.

We begin by representing the linear network as a graph  $(\mathcal{V}, \mathcal{E})$ , where the vertex set  $\mathcal{V} = \{v_1, \dots, v_n\}$  corresponds to the endpoints of  $\mathcal{L}$ , and the edge set  $\mathcal{E}$  corresponds to the linear segments  $\ell_1, \dots, \ell_m$ . The length of  $\ell_i$  is denoted by  $|\ell_i|$ . We write  $v_i \sim v_j$  if the distinct vertices  $v_i$  and  $v_j$  are connected by an edge. For any pair of vertices  $v_i, v_j \in \mathcal{V}$ , the conductance function is defined as

$$\text{con}(v_i, v_j) = \begin{cases} 1/\|v_i - v_j\|, & \text{if } v_i \sim v_j, \\ 0, & \text{otherwise.} \end{cases}$$

Using this function, we can build a matrix  $\Delta$  indexed by the vertices in  $\mathcal{V}$ , with entries

$$\Delta(v_i, v_j) = \begin{cases} 1 + c(v^*), & \text{if } v_i = v_j = v^*, \\ c(v_i), & \text{if } v_i = v_j \neq v^*, \\ -\text{con}(v_i, v_j), & \text{otherwise,} \end{cases}$$

where  $v^* \in \mathcal{V}$  is an arbitrary reference vertex and  $c(v_i) = \sum_{v \sim v_i} \text{con}(v_i, v)$ . The resulting matrix can be viewed as a modification of the graph Laplacian, where the inclusion of an additional unit term on the diagonal guarantees strict positive definiteness. This construction is invariant to the choice of  $v^*$  ([Anderes et al., 2020](#)).

To define the resistance metric, we introduce an auxiliary GRF on  $\mathcal{L}$ , given by

$$A(s) = A_0(s) + \sum_{i=1}^m A_i(s), \quad s \in \mathcal{L}, \quad (1)$$

where  $A_0, \dots, A_m$  are independent GRFs defined as follows:

- The base component  $A_0$  is first defined on the vertices as a multivariate normal vector:

$$(A_0(v_1), \dots, A_0(v_n))^\top \sim \mathcal{N}_n(\mathbf{0}, \Delta^{-1}).$$

Next,  $A_0$  is extended from the vertices to the edges using linear interpolation.

- For  $i = 1, \dots, m$ ,

$$A_i(s) = \begin{cases} B_i(s), & \text{for } s \in \ell_i, \\ 0, & \text{for } s \in \mathcal{L} \setminus \ell_i, \end{cases}$$

where  $B_1, \dots, B_m$  are independent standard Brownian bridges, each defined on an interval of length  $|\ell_i|$ , starting and ending at zero, and independent of  $A_0$ . Since each  $B_i$  is defined on an interval, writing  $B_i(s)$  implicitly identifies points  $s$  along  $\ell_i$  with points in this interval via arc length parameterization (see [Møller and Rasmussen, 2024](#) for further details).

The resistance metric on  $\mathcal{L}$  is defined as the variogram of the auxiliary GRF in Equation (1):

$$d_R(s, t) = \text{var}[A(s) - A(t)], \quad s, t \in \mathcal{L}. \quad (2)$$

This metric extends the classical resistance metric from electrical network theory (Klein and Randić, 1993), originally defined on the vertex set, to the continuum of points along the edges of the graph. When evaluated on any additional points along the edges,  $d_R$  coincides with the metric obtained from the corresponding discrete electrical network. Interestingly, the resistance and geodesic distances coincide when  $\mathcal{L}$  is a tree, that is, a connected graph with no cycles. Møller and Rasmussen (2024) provide more fully developed algebraic expressions for the resistance metric, which facilitate its implementation.

We turn to a description of the range of isotropic covariance functions attainable using the resistance metric. A function  $\varphi : [0, \infty) \rightarrow \mathbb{R}$  is said to be completely monotone on  $[0, \infty)$  if it is continuous on  $[0, \infty)$ , infinitely differentiable on  $(0, \infty)$ , and satisfies  $(-1)^j \varphi^{(j)}(z) \geq 0$ ,  $z > 0$ , for every integer  $j \geq 0$ , where  $\varphi^{(j)}$  denotes the  $j$ th derivative of  $\varphi$  and  $\varphi^{(0)} = \varphi$ . Anderes et al. (2020) showed that for any completely monotone function  $\varphi$ , the function  $K(s, t) = \varphi(d_R(s, t))$  is (strictly) positive definite on  $\mathcal{L} \times \mathcal{L}$ . As a consequence, many popular parametric classes of covariance functions developed for Euclidean spaces are also valid with respect to the resistance metric for general linear networks (see Anderes et al., 2020, Table 1).

In contrast, the geodesic distance provides a more restrictive alternative. For example, if  $\mathcal{L}$  contains three distinct paths connecting two points  $s, t \in \mathcal{L}$ , the classical exponential covariance function, defined with respect to the geodesic metric, is no longer positive definite on this network (Anderes et al., 2020).

In the context of point processes on linear networks, Møller and Rasmussen (2024) emphasize the advantages of the resistance metric over the geodesic metric in terms of modeling flexibility. In particular, the use of  $d_R$  allows one to model stronger clustering effects in Cox processes and higher degree of repulsiveness in determinantal point processes.

### 3. Non-stationary covariance functions

#### 3.1. Main result

We now present a general theorem for constructing non-stationary families of covariance functions on linear networks.

**Theorem 3.1.** *Let  $a : \mathcal{L} \rightarrow (0, \infty)$  and  $b : \mathcal{L} \rightarrow (0, \infty)$ , and define  $\alpha(s, t) = [a(s) + a(t)]/2$ . Let  $d_R(s, t)$  be the resistance metric between  $s$  and  $t$ , and let  $F$  be a positive finite measure on  $(0, \infty)$ . Then, the function*

$$K(s, t) = \int_0^\infty \frac{\sqrt{b(s)b(t)}}{\sqrt{\alpha(s, t) + d_R(s, t)}w} dF(w), \quad s, t \in \mathcal{L}, \quad (3)$$

*is positive semidefinite on  $\mathcal{L} \times \mathcal{L}$ .*

Our proof of Theorem 3.1, presented below, adapts ideas introduced in Paciorek (2003) for establishing positive definiteness of non-stationary covariance functions in Euclidean spaces. To the best of our knowledge, the present work is the first to extend this approach to linear networks. The fact that the resistance metric is defined as the variogram of a specific auxiliary GRF gives the proof a distinctive character.

**Proof.** A direct calculation shows that, for all  $w > 0$ ,

$$\begin{aligned} \frac{1}{\sqrt{\alpha(s, t) + d_R(s, t)w}} &= \frac{1}{\sqrt{\alpha(s, t)}} \int_{\mathbb{R}} \exp \left\{ -\frac{wd_R(s, t)y^2}{2\alpha(s, t)} \right\} \frac{1}{\sqrt{2\pi}} \exp \left\{ -\frac{y^2}{2} \right\} dy, \\ &= \frac{1}{\sqrt{\alpha(s, t)}} \mathbb{E} \left[ \exp \left\{ -\frac{wd_R(s, t)Y^2}{2\alpha(s, t)} \right\} \right], \end{aligned} \quad (4)$$

where the expectation in (4) is taken with respect to  $Y \sim \mathcal{N}(0, 1)$ . Consequently,  $K$  in Equation (3) can be written as

$$K(s, t) = \frac{\sqrt{b(s)b(t)}}{\sqrt{\alpha(s, t)}} \int_0^\infty \mathbb{E} \left[ \exp \left\{ -\frac{wd_R(s, t)Y^2}{2\alpha(s, t)} \right\} \right] dF(w), \quad s, t \in \mathcal{L}. \quad (5)$$

Let  $\phi(\cdot; \mu, \sigma^2)$  denote the probability density function of a normal distribution with mean  $\mu$  and variance  $\sigma^2$ . Using a convolution argument, we obtain

$$\int_{\mathbb{R}} \phi \left( \xi; \frac{A(s)}{\sqrt{2}}, \frac{a(s)}{4w} \right) \phi \left( \xi; \frac{A(t)}{\sqrt{2}}, \frac{a(t)}{4w} \right) d\xi = \frac{\sqrt{w}}{\sqrt{\pi\alpha(s, t)}} \exp \left\{ -\frac{w[A(s) - A(t)]^2}{2\alpha(s, t)} \right\}, \quad (6)$$

for every  $w > 0$ , with this expression conditioned on the values,  $A(s)$  and  $A(t)$ , of the auxiliary GRF defined in Equation (1).

Notice that  $A(s) - A(t) \sim \mathcal{N}(0, d_R(s, t))$  and, consequently,  $[A(s) - A(t)]/\sqrt{d_R(s, t)}$  is equal in distribution to  $Y \sim \mathcal{N}(0, 1)$ . Taking the expectation in (6) with respect to  $(A(s), A(t))^\top$ , we obtain

$$\mathbb{E} \left[ \int_{\mathbb{R}} \phi \left( \xi; \frac{A(s)}{\sqrt{2}}, \frac{a(s)}{4w} \right) \phi \left( \xi; \frac{A(t)}{\sqrt{2}}, \frac{a(t)}{4w} \right) d\xi \right] = \frac{\sqrt{w}}{\sqrt{\pi\alpha(s, t)}} \mathbb{E} \left[ \exp \left\{ -\frac{wd_R(s, t)Y^2}{2\alpha(s, t)} \right\} \right], \quad (7)$$

where the right-hand side of Equation (7) simplifies to an expectation with respect to  $Y \sim \mathcal{N}(0, 1)$ . Therefore, using Equation (7) and Fubini's theorem, the function  $K$  in Equation (5) can be written as

$$K(s, t) = \sqrt{\pi} \mathbb{E} \left[ \int_0^\infty \int_{\mathbb{R}} \sqrt{b(s)b(t)} \phi \left( \xi; \frac{A(s)}{\sqrt{2}}, \frac{a(s)}{4w} \right) \phi \left( \xi; \frac{A(t)}{\sqrt{2}}, \frac{a(t)}{4w} \right) d\xi w^{-1/2} dF(w) \right].$$

We conclude that for any  $N \in \mathbb{N}$ ,  $r_1, \dots, r_N \in \mathbb{R}$ , and  $s_1, \dots, s_N \in \mathcal{L}$ ,

$$\begin{aligned} \sum_{i=1}^N \sum_{j=1}^N r_i r_j K(s_i, s_j) &= \sum_{i=1}^N \sum_{j=1}^N r_i r_j \sqrt{\pi} \mathbb{E} \left[ \int_0^\infty \int_{\mathbb{R}} \sqrt{b(s_i)b(s_j)} \phi \left( \xi; \frac{A(s_i)}{\sqrt{2}}, \frac{a(s_i)}{4w} \right) \right. \\ &\quad \left. \phi \left( \xi; \frac{A(s_j)}{\sqrt{2}}, \frac{a(s_j)}{4w} \right) d\xi w^{-1/2} dF(w) \right], \end{aligned}$$

that is,

$$\sum_{i=1}^N \sum_{j=1}^N r_i r_j K(s_i, s_j) = \sqrt{\pi} \mathbb{E} \left[ \int_0^\infty \int_{\mathbb{R}} \left\{ \sum_{i=1}^N r_i \sqrt{b(s_i)} \phi \left( \xi; \frac{A(s_i)}{\sqrt{2}}, \frac{a(s_i)}{4w} \right) \right\}^2 d\xi w^{-1/2} dF(w) \right] \geq 0.$$

Therefore,  $K$  is positive semidefinite. □

Observe that if  $s$  and  $t$  are near a fixed location  $s_0 \in \mathcal{L}$ , and both functions  $b$  and  $a$  are sufficiently smooth, then

$$K(s, t) \approx \int_0^\infty \frac{b(s_0)}{\sqrt{a(s_0) + d_R(s, t)w}} dF(w).$$

In other words,  $K(s, t)$  depends approximately only on the resistance metric  $d_R(s, t)$ . This property allows us to construct covariance models with locally isotropic behavior with respect to  $d_R$ , reflecting the topology of the linear network.

In this framework, the function  $b$  provides a way to modulate the locally varying variance of the field, while the function  $a$  regulates how quickly the covariance decreases with distance. In particular,  $a$  can be adjusted to influence the locally adaptive correlation range (the distance beyond which correlations fall below 0.05).

### 3.2. Examples

A direct calculation shows that  $K(s, t)$  in Equation (3) can be written as

$$K(s, t) = \begin{cases} \frac{b(s)}{\sqrt{a(s)}} F((0, \infty)), & \text{if } s = t, \\ \sqrt{\frac{b(s)b(t)}{d_R(s, t)}} \psi\left(\frac{\alpha(s, t)}{d_R(s, t)}\right), & \text{if } s \neq t, \end{cases}$$

where

$$\psi(r) = \int_0^\infty \frac{1}{\sqrt{r+w}} dF(w), \quad r > 0. \quad (8)$$

Functions of the form (8) belong to the class of generalized Stieltjes functions of order 1/2 (see, e.g., [Koumandos and Pedersen, 2019](#)). When  $a$  and  $b$  are constant functions, we recover a subclass of the isotropic covariance functions presented in [Anderes et al. \(2020\)](#), since every generalized Stieltjes function is completely monotone (see, e.g., [Menegatto, 2020](#), Section 2.2).

Since closed-form expressions for generalized Stieltjes functions are available in standard tables of integral transforms such as ([Erdélyi, 1954](#), Chapter 14), it is straightforward to derive explicit examples of non-stationary covariance functions.

**Example 3.1.** Let  $F$  be the Dirac delta measure at  $\beta > 0$ , that is,  $dF(w) = d\delta_\beta(w)$ . Then, we immediately obtain the covariance function

$$K(s, t) = \sqrt{\frac{b(s)b(t)}{\alpha(s, t)}} \left(1 + \frac{\beta d_R(s, t)}{\alpha(s, t)}\right)^{-1/2}. \quad (9)$$

**Example 3.2.** Let  $dF(w) = (1/\beta) \exp(-w/\beta) dw$ , for  $\beta > 0$ . Then, using Equation 14.4.10 in [Erdélyi \(1954\)](#), we obtain

$$K(s, t) = \begin{cases} \frac{b(s)}{\sqrt{a(s)}}, & \text{if } s = t, \\ \sqrt{\frac{\pi b(s)b(t)}{\beta}} \exp\left(\frac{\alpha(s, t)}{\beta d_R(s, t)}\right) \operatorname{erfc}\left(\sqrt{\frac{\alpha(s, t)}{\beta d_R(s, t)}}\right), & \text{if } s \neq t, \end{cases}$$

where  $\text{erfc}$  denotes the complementary error function.

**Example 3.3.** Let  $dF(w) = \sqrt{\beta}\pi^{-1}w^{-1/2}(\beta + w)^{-1}dw$ , for  $\beta > 0$ . This is a scaled Beta prime probability measure. Then, using Equation 14.4.9 in [Erdélyi \(1954\)](#), we obtain

$$K(s, t) = \begin{cases} \frac{b(s)}{\sqrt{a(s)}}, & \text{if } s = t, \\ \frac{2}{\pi} \sqrt{\frac{b(s)b(t)}{\beta}} {}_2F_1 \left( 1, 1/2, 3/2; 1 - \frac{\alpha(s, t)}{\beta d_R(s, t)} \right), & \text{if } s \neq t, \end{cases}$$

where  ${}_2F_1$  denotes the Gauss hypergeometric function.

### 3.3. Illustration

To illustrate our proposal, we simulate a GRF on a linear network formed by the mortar lines of a brick wall. This network, consisting of 156 vertices and 203 edges, and available in the R package `spatstat` ([Baddeley and Turner, 2005](#)), has been the focus of studies on the positions of spider webs of the urban wall spider *Oecobius navus* ([Voss et al., 2007](#)).

We use the covariance function in Equation (9) with  $\beta = 1$  and the parameterization  $b(s) = c(s)\sqrt{a(s)}$ , for some function  $c : \mathcal{L} \rightarrow (0, \infty)$ , which ensures that  $\text{var}[X(s)] = K(s, s) = c(s)$ , for all  $s \in \mathcal{L}$ . Specifically, we consider

$$a(s) = 2500 \times \exp \left( -\frac{d_R(s, s^*)}{100} \right), \quad s \in \mathcal{L}, \quad (10)$$

and

$$c(s) = 2 \times \exp \left( -\frac{d_R(s, s^*)}{1000} \right), \quad s \in \mathcal{L}, \quad (11)$$

where  $s^*$  is a fixed point on  $\mathcal{L}$ . Both functions attain their maximum at  $s^*$  and decay exponentially as  $s$  moves away from this point, as illustrated in Figure 1. Accordingly, we expect the simulated GRF to exhibit larger correlation range and higher variance at locations near  $s^*$ , decreasing as one moves away from this point.

To better illustrate the local behavior of this covariance function, Figure 2 shows the curves  $d_R \mapsto \sqrt{a_0}/\sqrt{a_0 + d_R}$  for different values of  $a_0$ . These curves capture part of the local isotropic correlation structures that the covariance function exhibits. They are displayed over the interval  $(0, 800)$  since the maximum resistance distance between two points in this domain is approximately 837.

Figure 3 (left panel) shows the simulated GRF over 5,684 sites (28 per edge). The field attains high values at sites in the top part of the linear network, and because the correlation range is greater in this region, these high values extend over a wide area. In contrast, at sites in the lower part of the linear network, the field varies more rapidly, reflecting a smaller correlation range.

The right panel of Figure 3 shows the realization of the corresponding LGCP, where the log Gaussian random field is defined as  $\Lambda(s) = 0.002 \times \exp\{X(s)\}$ , with  $X(s)$  denoting the underlying GRF. Recall that, conditioned on  $\Lambda$ , this point process on  $\mathcal{L}$  is almost surely a Poisson process with intensity function  $\Lambda$  (with respect to the arc length measure on  $\mathcal{L}$ ). As expected, more points occur

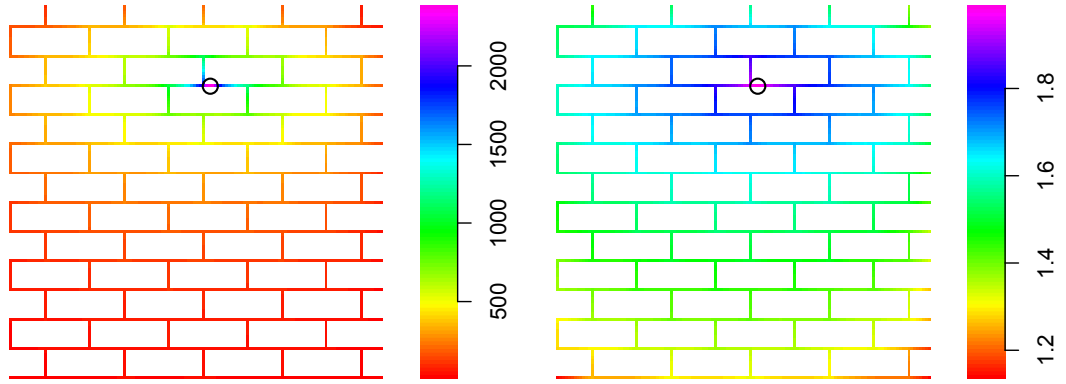


Figure 1: Functions  $a$  (left) and  $c$  (right), defined in Equations (10) and (11), respectively, on the `spiders` linear network. The circle indicates the point  $s^*$  involved in the definitions of  $a$  and  $c$ .

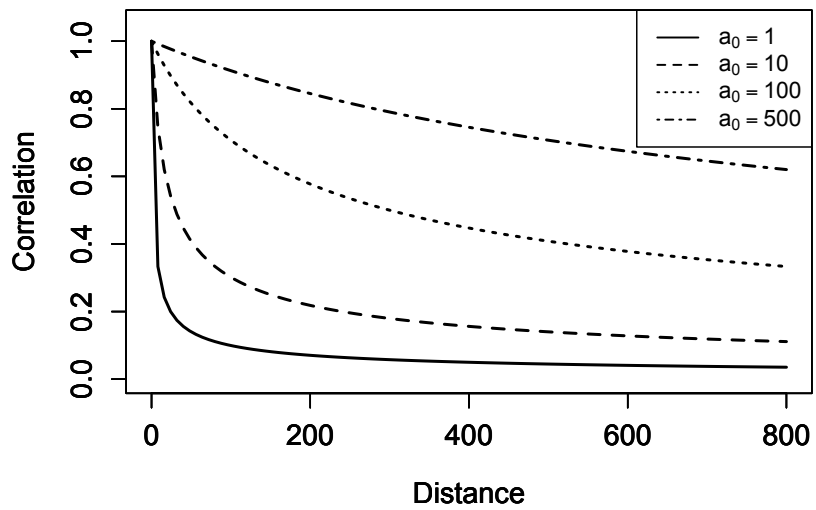


Figure 2: Mapping  $d_R \mapsto \sqrt{a_0}/\sqrt{a_0 + d_R}$  for selected values of  $a_0$ , illustrating how the local isotropic correlation structure depends on  $a_0$ .

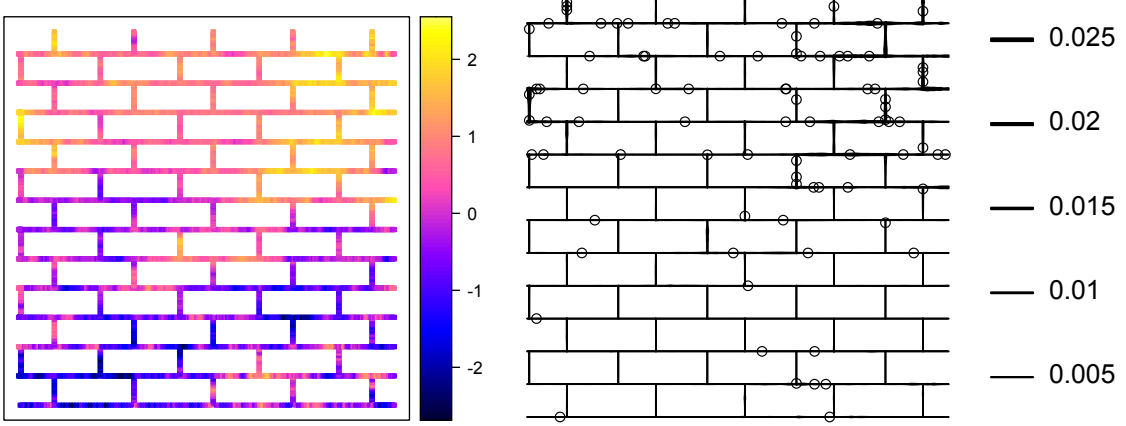


Figure 3: (Left) Simulated GRF on the `spiders` linear network, with the non-stationary covariance function given in Equation (9). (Right) Corresponding realization of a LGCP, with line thickness proportional to the magnitude of the log Gaussian field.

in the upper part of the network, covering a larger area, while fewer points are present in the lower part.

For a more detailed treatment of Cox processes on linear networks, we refer the reader to [Møller and Rasmussen \(2024\)](#).

#### 4. Weighted local likelihood

##### 4.1. Description of the method

We consider the weighted local likelihood estimation proposed by [Anderes and Stein \(2011\)](#). We now describe the method and the necessary modifications required to adapt it to the network context.

Suppose that we observe a realization of a GRF  $\{X(s) : s \in \mathcal{L}\}$  at locations  $s_1, \dots, s_N$  in  $\mathcal{L}$ . For any given site  $s \in \mathcal{L}$ , let  $\mathcal{N}_{s,k}$  denote the set of  $k$  observations nearest to  $s$  with respect to the resistance metric. Recall that our goal is to estimate  $a$  and  $b$  at the selected site  $s$ . Given weights  $\lambda_1, \dots, \lambda_N$ , the weighted local likelihood function is defined as

$$\mathcal{W}(a_0, b_0 | X(s_1), \dots, X(s_N)) = \sum_{k=1}^N \lambda_k [\text{Lik}(a_0, b_0 | \mathcal{N}_{s,k}) - \text{Lik}(a_0, b_0 | \mathcal{N}_{s,k-1})],$$

where  $\text{Lik}(a_0, b_0 | \mathcal{N}_{s,k})$  denotes the log-likelihood of the data in  $\mathcal{N}_{s,k}$ , with  $a_0$  and  $b_0$  representing fixed values of the functions  $a(\cdot)$  and  $b(\cdot)$ . As in [Anderes and Stein \(2011\)](#), we define  $\text{Lik}(a_0, b_0 | \mathcal{N}_{s,0})$  as 0.

The local estimate of  $(a(s), b(s))$  is given by

$$(\hat{a}(s), \hat{b}(s)) = \arg \max_{(a_0, b_0)} \mathcal{W}(a_0, b_0 \mid X(s_1), \dots, X(s_N)).$$

The principle behind this method is that we locally fit an isotropic model, not simply by taking a window of data around  $s$  (a strategy also used in [Anderes and Stein, 2011](#), which has been shown to be less competitive), but by considering inflating neighborhoods and gradually assigning less weight to those that cover a very large region. For this reason, the weights include a bandwidth parameter to control this effect.

#### 4.2. Simulation study

In our simulation experiments, we focus on two main aspects. First, we study the performance of the weighted local likelihood method in the linear network setting, where it has not been previously examined. Second, we evaluate both the statistical and computational performance of compactly supported weights  $\lambda_k^{\text{cs}}$  in comparison with Gaussian weights  $\lambda_k^{\text{g}}$ .

Specifically, we consider the following weighting schemes:

$$\lambda_k^{\text{cs}} = \left( 1 - \frac{d_R(s, s_k)}{\tau} \right)_+, \quad k = 1, \dots, N, \quad (12)$$

where  $(r)_+ = \max\{0, r\}$  denotes the positive part function, and

$$\lambda_k^{\text{g}} = \exp\left(-\frac{d_R(s, s_k)^2}{\eta^2}\right), \quad k = 1, \dots, N, \quad (13)$$

where we assume that the sites  $s_1, \dots, s_N$  are ordered by their distance to  $s$ , for simplicity. Here,  $\tau$  and  $\eta$  are bandwidth parameters. Because compactly supported weights vanish beyond a certain distance when the bandwidth is moderate, only a subset of the neighborhoods  $\mathcal{N}_{s,1}, \dots, \mathcal{N}_{s,N}$  may contribute to the local likelihood at  $s$ , which can reduce the computational cost.

We consider the [Chicago](#) street network available in the [R](#) package [spatstat](#), and the covariance function in Equation (9), with the parameterization discussed in Section 3.3. Following [Anderes and Stein \(2011\)](#), we assume for simplicity that the variance of the random field is known and equal to one, so that we focus on the estimation of the local practical range. The function  $a$  used in our study is shown in the left panel of Figure 4. We also highlight six randomly selected locations on the network at which  $a$  will be estimated.

We simulate 100 independent realizations of the GRF on this domain at 503 locations (one at the midpoint of each edge). For each realization, we estimate  $a$  at the six selected sites. The weighted local likelihood method is implemented with the weighting schemes described above. We use bandwidth parameters  $\eta = 120$  and  $\tau = 200$ , which produce weight functions with a comparable spatial extent but distinct structural features (see the right panel of Figure 4). For reference, the maximum resistance distance between two points in this network is approximately 675.

In Figure 5, we show the centered boxplots of the estimates across the 100 realizations, for each weighting scheme and each of the six selected sites. Overall, no significant bias is observed in any of the boxplots, demonstrating the effectiveness of the method. One point of interest is the higher variance in the estimates at site 2. This effect is consistent with the site's proximity to the

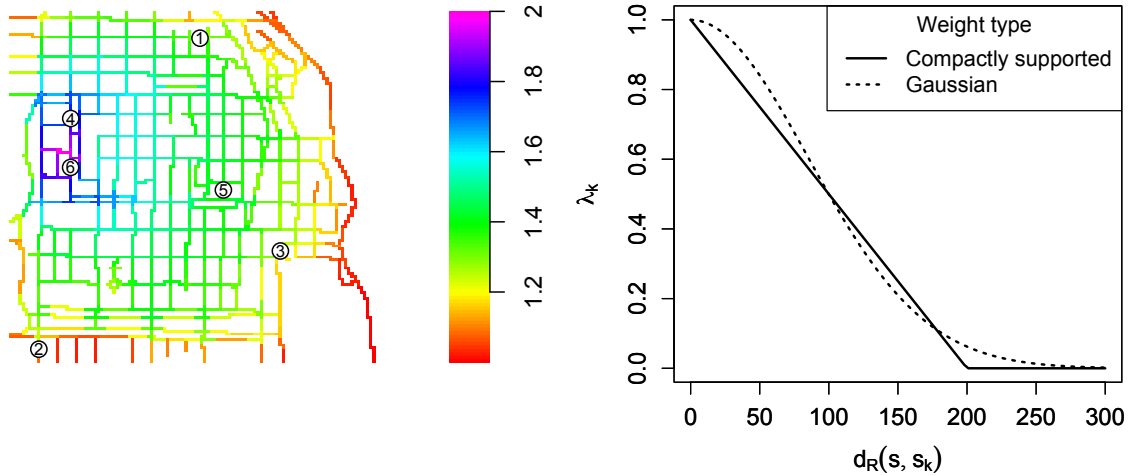


Figure 4: (Left) The function  $a$  used in our simulations on the Chicago street network. Six randomly selected locations where  $a$  will be estimated are highlighted. (Right) Decay of the weights as a function of the resistance metric for the compactly supported ( $\tau = 120$ ) and Gaussian ( $\eta = 120$ ) weighting schemes.

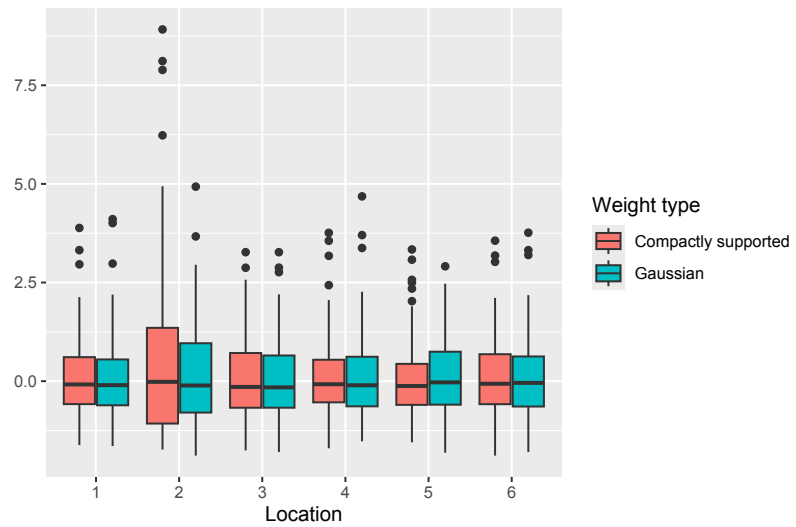


Figure 5: Centered boxplots of the estimates of  $a$ , at the six selected sites, across 100 independent realizations of a GRF with covariance function (9). Results are shown for the compactly supported and Gaussian weighting schemes.

Table 1: Times (in seconds) for a single evaluation of the weighted local likelihood function under each weighting scheme, as a function of the sample size  $N$ . For the compactly supported weights we consider  $\tau = 100, 150$ , and  $200$ . The simulation was performed on an Apple M1 chip with 8GB of memory.

	$N = 503$	$N = 1006$	$N = 1509$	$N = 2012$
Compactly supported ( $\tau = 100$ )	0.046	0.322	1.348	5.037
Compactly supported ( $\tau = 150$ )	1.056	20.39	107.8	372.7
Compactly supported ( $\tau = 200$ )	2.009	35.41	196.7	648.6
Gaussian	2.257	41.35	225.8	759.0

boundary of the network, which reduces the number of neighbors that effectively contributes to the local estimate. A similar observation was reported by [Anderes and Stein \(2011\)](#).

Next, we comment on the comparison between the two types of weights. We observe similar results for both approaches, with a slight advantage for the compactly supported weights in terms of variance at sites 4, 5, and 6. However, at the boundary site 2, the variance is more pronounced when using compactly supported weights. Overall, compactly supported weights appear to be competitive from a statistical perspective.

We also compare the computational performance of the weighting schemes by measuring evaluation times as a function of the sample size of the GRF. Specifically, we simulate GRFs with  $N = 503, 1006, 1509$ , and  $2012$ , which correspond to taking 1, 2, 3, and 4 locations per edge, respectively, and implement the method using compactly supported weights with bandwidth parameters  $\tau = 100, 150$ , and  $200$ . For each configuration, we report the time required for a single evaluation of the weighted local likelihood function. The results are summarized in Table 1, allowing us to assess the computational gains relative to the Gaussian weighting scheme. For  $\tau = 100$  and  $150$ , the reduction in computation time is particularly pronounced. For instance, when  $\tau = 150$ , the computation time is reduced by approximately 50% compared with Gaussian weighting scheme, whereas for  $\tau = 100$ , evaluating the objective function takes at most 2% of the time required with Gaussian weights, and for most sample sizes the percentage is even lower.

Our findings both support the observations reported in [Anderes and Stein \(2011\)](#) regarding reduced precision near the domain boundaries and provide additional insights into the statistical and computational performance of different weighting schemes in our specific setting. A promising strategy is to use a combination of weights, employing compactly supported weights in the interior and adapting the weights near the boundaries. We refer the reader to [Anderes and Stein \(2011\)](#) for a more comprehensive treatment of weights and bandwidth selection.

## 5. Discussion

This paper proposes non-stationary covariance functions for random fields defined on linear networks. The models exhibit local isotropy with respect to the resistance metric, allowing both the variance and correlation range to vary spatially. We demonstrate the effectiveness of a weighted local likelihood approach with compactly supported weights for estimating the proposed models, which provide a balance between computational efficiency and statistical accuracy.

Although constructive criticism has been raised regarding covariance models based on the resistance metric ([Bolin et al., 2024](#)), primarily because existing covariance families under this metric do not

provide explicit control over the mean-square differentiability of the random field (i.e., there is no direct analogue of the Matérn covariance model under the resistance metric), we argue that the models introduced in this work offer considerable potential for practical applications. In the context of point process modeling, and in particular for LGCPs, local flexibility in variance and correlation range is essential for capturing heterogeneous aggregation structures, even when the smoothness level of the latent GRF is kept fixed (Dvořák et al., 2019). The proposed models are also applicable to geostatistical data, such as continuous measurements along stream networks. Since they do not allow control over the smoothness of the random field, their applicability is limited to phenomena exhibiting relatively rough variations across space. Extending the framework to include flexible smoothness represents a promising direction for future research.

Other strategies for modeling non-stationarity in Euclidean spaces, such as domain deformation or kernel convolutions of isotropic random fields, could potentially be adapted to linear networks (see Schmidt and Guttorp, 2020 and references therein). Investigating these approaches represents a promising direction for future research.

Another interesting avenue is the development of nonparametric and semiparametric estimation methods in the network setting, analogous to the approaches of Chang et al. (2010) and Kidd and Katzfuss (2022) in Euclidean spaces, as well as the design of fast geostatistical simulation algorithms by adapting the ideas in Alegría et al. (2026).

## Acknowledgement

Alfredo Alegría is partially supported by the National Agency for Research and Development of Chile through grant ANID Fondecyt 1251154.

## References

Alegría, A., Emery, X., Filosi, T., Porcu, E., 2026. Computationally efficient algorithms for simulating isotropic Gaussian random fields on graphs with euclidean edges. *Journal of Computational and Graphical Statistics* forthcoming. doi:[10.1080/10618600.2025.2574535](https://doi.org/10.1080/10618600.2025.2574535).

Anderes, E., Møller, J., Rasmussen, J.G., 2020. Isotropic covariance functions on graphs and their edges. *The Annals of Statistics* 48, 2478–2503.

Anderes, E.B., Stein, M.L., 2011. Local likelihood estimation for nonstationary random fields. *Journal of Multivariate Analysis* 102, 506–520.

Baddeley, A., Nair, G., Rakshit, S., McSwiggan, G., 2017. “stationary” point processes are uncommon on linear networks. *Stat* 6, 68–78.

Baddeley, A., Nair, G., Rakshit, S., McSwiggan, G., Davies, T.M., 2021. Analysing point patterns on networks—A review. *Spatial Statistics* 42, 100435.

Baddeley, A., Turner, R., 2005. Spatstat: an r package for analyzing spatial point patterns. *Journal of statistical software* 12, 1–42.

Bolin, D., Riera-Segura, L., Simas, A.B., 2025. A new class of non-stationary gaussian fields with general smoothness on metric graphs. *arXiv preprint arXiv:2501.11738* .

Bolin, D., Simas, A.B., Wallin, J., 2024. Gaussian Whittle–Matérn fields on metric graphs. *Bernoulli* 30, 1611–1639.

Chang, Y.M., Hsu, N.J., Huang, H.C., 2010. Semiparametric estimation and selection for non-stationary spatial covariance functions. *Journal of Computational and Graphical Statistics* 19, 117–139.

Cox, D.R., 1955. Some statistical methods connected with series of events. *Journal of the Royal Statistical Society: Series B (Methodological)* 17, 129–157.

Cronie, O., Moradi, M., Mateu, J., 2020. Inhomogeneous higher-order summary statistics for point processes on linear networks. *Statistics and Computing* 30, 1221–1239.

Dvořák, J., Møller, J., Mrkvička, T., Soubeyrand, S., 2019. Quick inference for log Gaussian Cox processes with non-stationary underlying random fields. *Spatial Statistics* 33, 100388.

Erdélyi, A., 1954. Tables of Integral Transforms, Volume II. McGraw-Hill, New York.

González-Pérez, I., Borrajo, M.I., González-Manteiga, W., 2025. Nonparametric testing of first-order structure in point processes on linear networks. *Statistical Papers* 66, 42.

Kidd, B., Katzfuss, M., 2022. Bayesian nonstationary and nonparametric covariance estimation for large spatial data (with discussion). *Bayesian Analysis* 17, 291–351.

Kleiber, W., Nychka, D., 2012. Nonstationary modeling for multivariate spatial processes. *Journal of Multivariate Analysis* 112, 76–91.

Klein, D., Randić, M., 1993. Resistance distance. *Journal of Mathematical Chemistry* 12, 81–95.

Koumandos, S., Pedersen, H.L., 2019. On generalized Stieltjes functions. *Constructive Approximation* 50, 129–144.

Liang, M., Marcotte, D., 2016. A class of non-stationary covariance functions with compact support. *Stochastic Environmental Research and Risk Assessment* 30, 973–987.

Mateu, J., Fernández-Avilés, G., Montero, J.M., 2013. On a class of non-stationary, compactly supported spatial covariance functions. *Stochastic Environmental Research and Risk Assessment* 27, 297–309.

Menegatto, V., 2020. Positive definite functions on products of metric spaces via generalized Stieltjes functions. *Proceedings of the American Mathematical Society* 148, 4781–4795.

Møller, J., Rasmussen, J.G., 2024. Cox processes driven by transformed Gaussian processes on linear networks—A review and new contributions. *Scandinavian Journal of Statistics* 51, 1288–1322.

Moradi, M., Mateu, J., 2020. First-and second-order characteristics of spatio-temporal point processes on linear networks. *Journal of Computational and Graphical Statistics* 29, 432–443.

Moradi, M., Sharifi, A., 2024. Summary statistics for spatio-temporal point processes on linear networks. *Spatial Statistics* 61, 100840.

Paciorek, C.J., 2003. Nonstationary Gaussian processes for regression and spatial modeling. Ph.D. thesis, Carnegie Mellon University.

Paciorek, C.J., Schervish, M.J., 2006. Spatial modelling using a new class of nonstationary covariance functions. *Environmetrics* 17, 483–506.

Porcu, E., White, P.A., Genton, M.G., 2023. Stationary nonseparable space-time covariance functions on networks. *Journal of the Royal Statistical Society Series B: Statistical Methodology* 85, 1417–1440.

Schmidt, A.M., Guttorp, P., 2020. Flexible spatial covariance functions. *Spatial Statistics* 37, 100416.

Ver Hoef, J.M., Peterson, E.E., 2010. A moving average approach for spatial statistical models of stream networks. *Journal of the American Statistical Association* 105, 6–18.

Voss, S.C., Main, B.Y., Dadour, I.R., 2007. Habitat preferences of the urban wall spider *oecobius navus* (araneae, oecobiidae). *Australian Journal of Entomology* 46, 261–268.

Yaglom, A.M., 1987. Correlation theory of stationary and related random functions, Volume I: Basic results. volume 1. Springer.